

Supplementary Information

Conversion of Ternary Zn_2SnO_4 Octahedrons into Binary Mesoporous SnO_2 and Hollow SnS_2 Hierarchical Ones by Template-Engaged Selective Complex-Extracted Route

Ping Cai, De-Kun Ma,* Quan-Cheng Liu, Shu-Mei Zhou, Wei Chen, and Shao-Ming Huang*

Nanomaterials and Chemistry Key Laboratory, Wenzhou University, Wenzhou, Zhejiang 325027, P. R. China

Experimental part

I. Synthesis of irregular Zn_2SnO_4 particles: 1 mmol of Zn $(\text{CH}_3\text{COO})_2$ was dissolved into 40 mL of ultrapure water under stirring. Then 1 mmol of Na_2SnO_3 and 15 mmol of NaOH were added into the solution. Subsequently, the solution was poured into a stainless steel autoclave with a Teflon liner of 50 mL capability and heated at 180 °C for 12 h. After the autoclave was cooled to room temperature, the resulting white precipitations were separated centrifugally and washed by diluted hydrochloric acid (pH= 2.50), deionized water, and absolute ethanol for several times. The products were dried at 60 °C for 4 h under vacuum for further characterization.

II. Synthesis of SnO_2 nanoparticles through solid-state reaction: 5 mmol of $\text{SnCl}_4 \cdot 5\text{H}_2\text{O}$ and 20 mmol of NaOH powders were mixed and ground together. Then they were put into a porcelain boat and reacted at 300 °C for 10 h in air. After the porcelain boat naturally cooled to room temperature, the resultant products were washed by ultrapure water and absolute ethanol for several times. After that, the products were dried at 60 °C for 4 h under vacuum for further characterization.

III. Synthesis of SnS_2 flowers through solid-state reaction: 5 mmol of SnCl_2 and 20 mmol of thiourea powders were mixed and ground together. Then they were put into a porcelain boat and reacted at 400 °C for 5 h under an Ar atmosphere. After the porcelain boat naturally cooled to room temperature, the resultant products were washed by ultrapure water and absolute ethanol for several times. Then, the products were dried at 60 °C for 4 h under vacuum for further characterization.

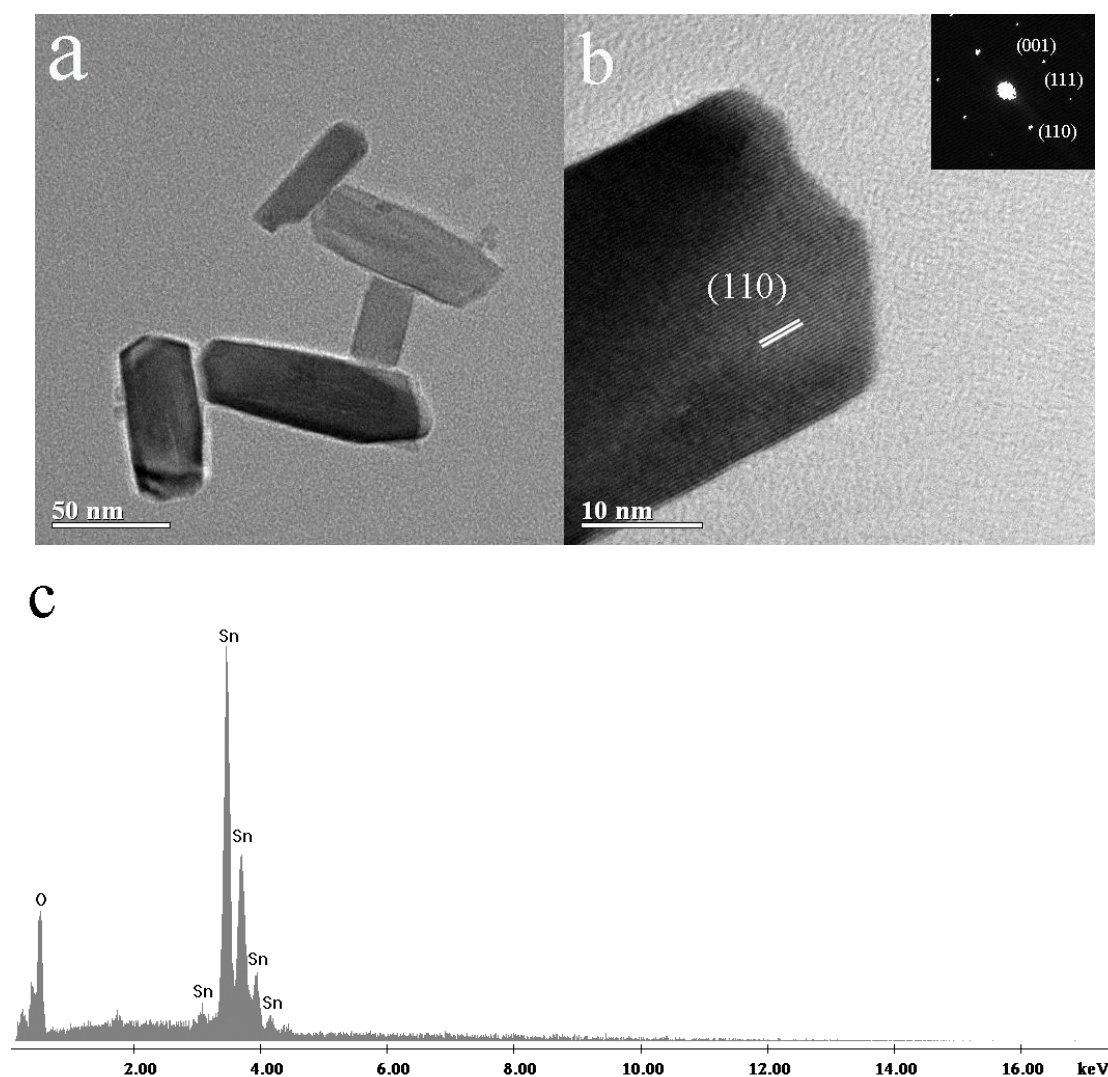


Figure S1. (a) TEM image of Zn₂SnO₄ octahedrons after strong ultrasonic treatment. (b) HRTEM image of a single Zn₂SnO₄ nanorod; the inset is corresponding SAED pattern recorded on the nanorod. (c) EDX spectrum of Zn₂SnO₄ octahedrons.

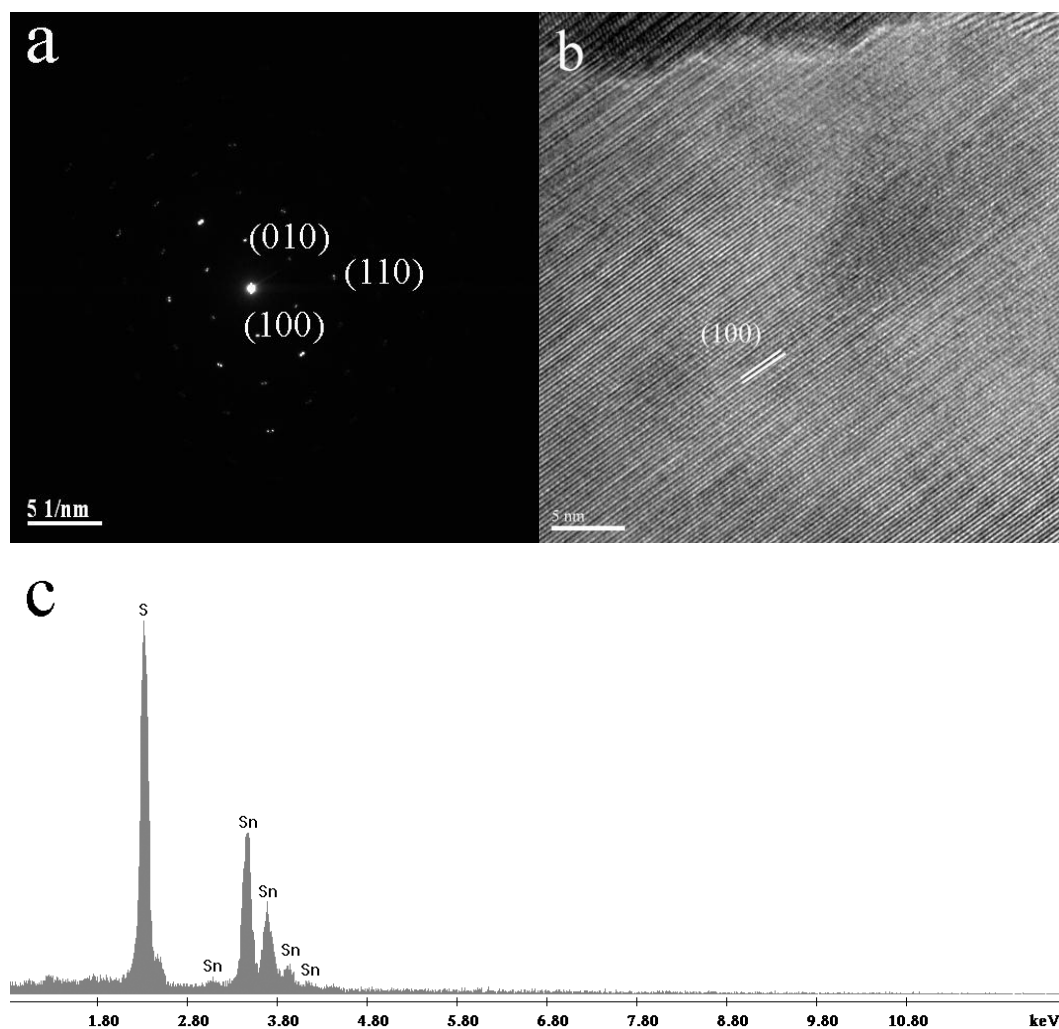


Figure S2. SAED pattern (a) and HRTEM image (b) recorded on an individual SnS_2 nanosheet. (c) EDX spectrum of SnS_2 octahedrons.

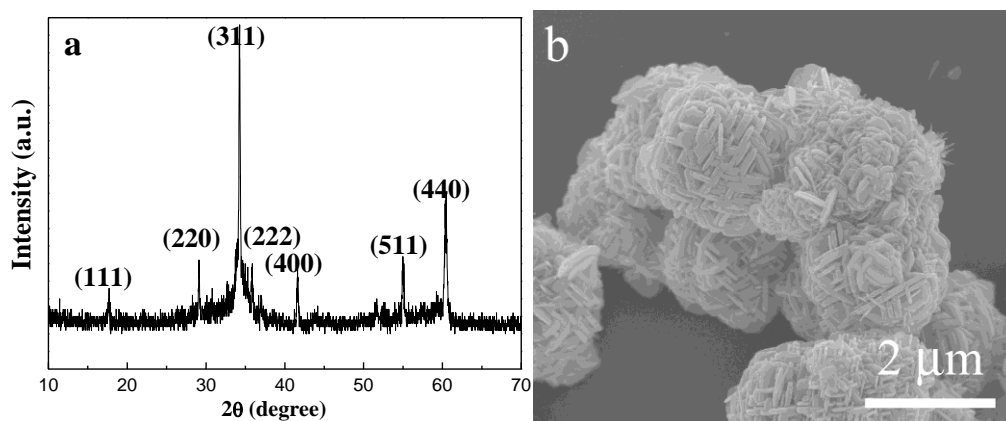


Figure S3. XRD pattern (a) and FE-SEM image (b) of the products synthesized through one-pot route, employing $\text{Zn}(\text{CH}_3\text{COO})_2$, Na_2SnO_3 , NaOH , and H_4EDTA as reaction reagents.

The XRD pattern of the as-synthesized products can be indexed to pure cubic-phase Zn_2SnO_4 (JCPDS no. 74-2184). FE-SEM image shows that the products consist of hierarchical reel of thread-like architectures assembled from nanoplates.

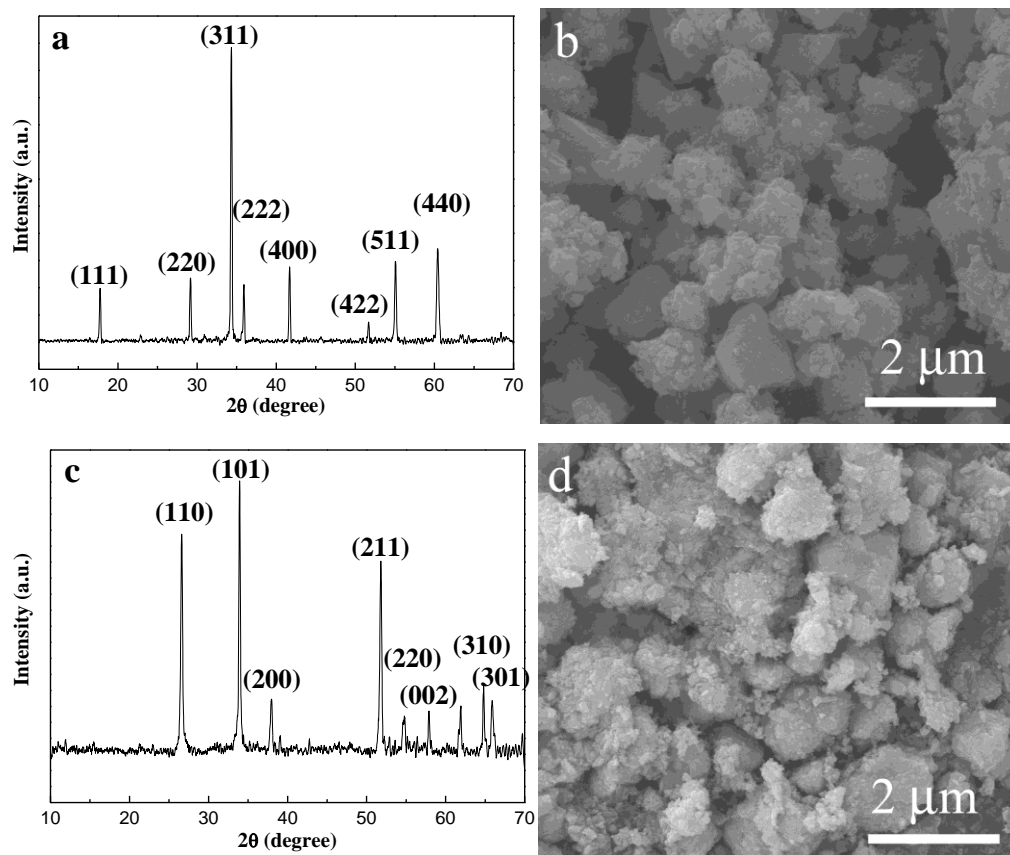


Figure S4. XRD pattern (a) and FE-SEM image (b) of the products synthesized at 180 °C for 12 h. XRD pattern (c) and (d) FE-SEM image of the products obtained through replacing Zn_2SnO_4 octahedrons with irregular Zn_2SnO_4 particles.

The XRD pattern of the as-synthesized products can be indexed to cubic-phase Zn_2SnO_4 (JCPDS no. 74-2184). From EF-SEM image of the corresponding products, it can be seen that the products are irregular particles. The XRD pattern shown in Figure S4c can be indexed to tetragonal-phase SnO_2 (JCPDS no. 88-0287). After the chemical conversion, irregular Zn_2SnO_4 particles change to irregular SnO_2 particles (Figure S4d).

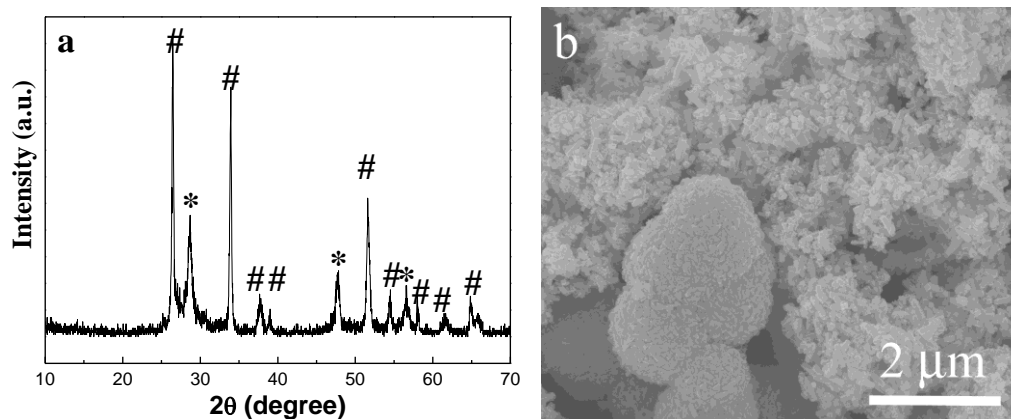


Figure S5. XRD pattern (a) and FE-SEM image (b) of the products synthesized through one-pot route, employing Zn(CH₃COO)₂, Na₂SnO₃, NaOH, H₄EDTA, and thioacetamide as reaction reagents.

XRD pattern of the products can be indexed to tetragonal-phase SnO₂ (denoted as #, JCPDS no. 88-0287) and hexagonal-phase ZnS (denoted as *, JCPDS no. 89-2739). FE-SEM image shows that the products consist of short nanorods and microspheres. No hierarchical SnS₂ octahedrons were obtained.

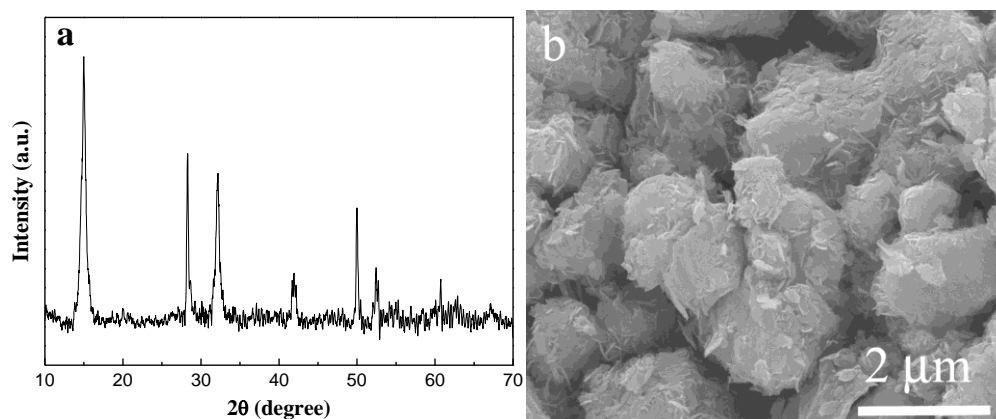


Figure S6. XRD pattern (a) and FE-SEM image (b) of the products synthesized at 200 °C for 8 h, using irregular Zn₂SnO₄ particles, H₄EDTA, and thioacetamide as reaction reagents.

XRD pattern of the resultant products can be indexed to pure hexagonal-phase SnS₂ (JCPDS no. 89-3198). FE-SEM image shows that the products consist of irregular hierarchical microspheres built by nanosheets.

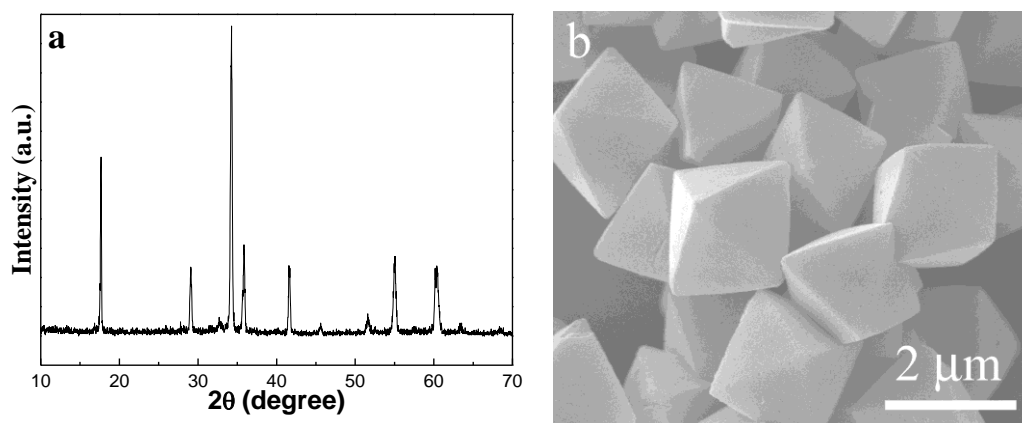


Figure S7. XRD pattern (a) and FE-SEM image (b) of Zn_2SnO_4 octahedrons hydrothermally treated in the absence of H_4EDTA .

The XRD pattern of the resultant products can be indexed to cubic-phase Zn_2SnO_4 (JCPDS no. 74-2184). From EF-SEM image of the corresponding products, it can be seen that the products consist of octahedral microcrystals.

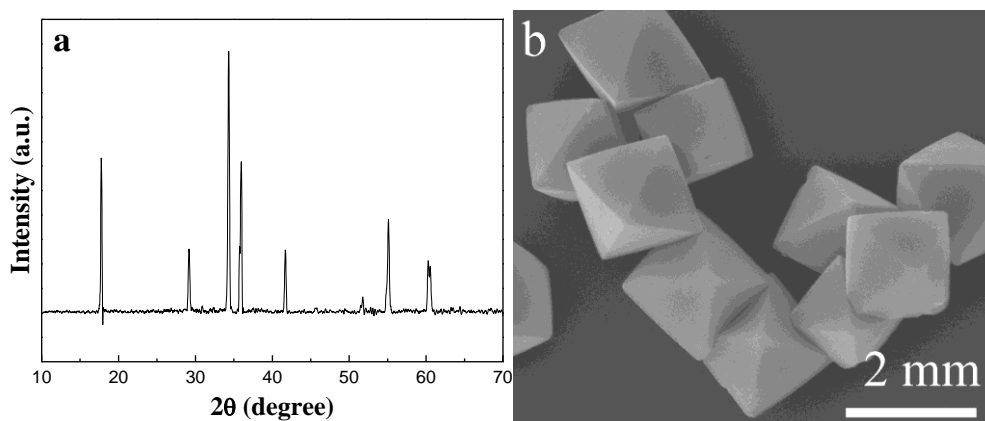


Figure S8. XRD pattern (a) and FE-SEM image (b) of Zn_2SnO_4 octahedrons hydrothermally treated under acid condition ($\text{pH}= 2.5$).

The XRD pattern of the resultant products can be indexed to pure cubic-phase Zn_2SnO_4 (JCPDS no. 74-2184). From EF-SEM image of the corresponding products, it can be seen that the products still consist of octahedral microcrystals.

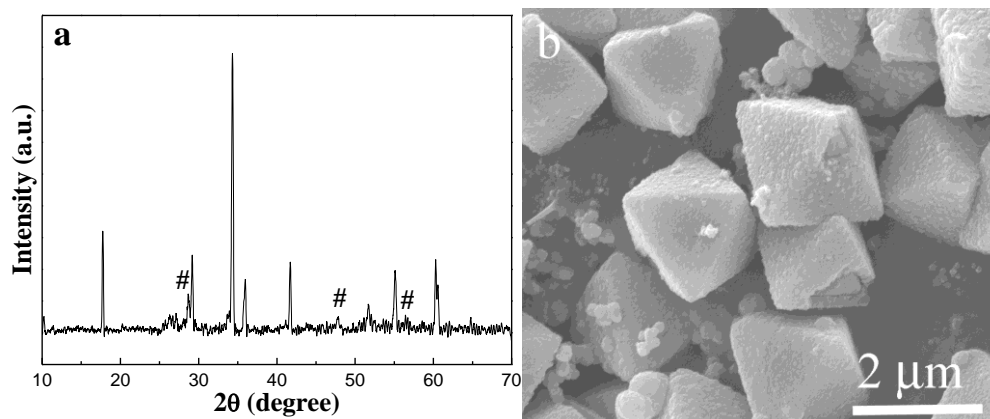


Figure S9. XRD pattern (a) and FE-SEM image (b) of the products synthesized with Zn_2SnO_4 octahedrons and TTA.

The XRD pattern of the resultant products can be indexed to main cubic-phase Zn_2SnO_4 (JCPDS no. 74-2184) and a small quantity of hexagonal-phase ZnS (denoted as #, JCPDS no. 89-2739). From EF-SEM image of the corresponding products, it can be seen that the products consist of octahedral microcrystals with core-shell structures.

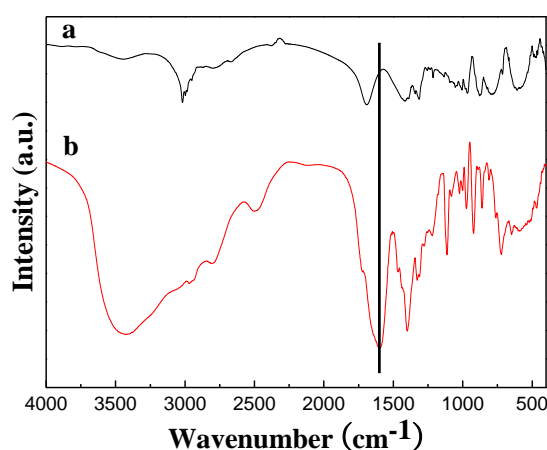


Figure S10. FT-IR spectra of (a) pure H_4EDTA and (b) H_4EDTA after hydrothermal reaction with Zn_2SnO_4 octahedrons.

As shown in Figure S10a, the characteristic vibration peak of carboxyl in H_4EDTA is located at 1691 cm^{-1} . After hydrothermal reaction with Zn_2SnO_4 octahedrons, the characteristic vibration peak of carboxyl was red shifted to 1610 cm^{-1} (Figure S10b).

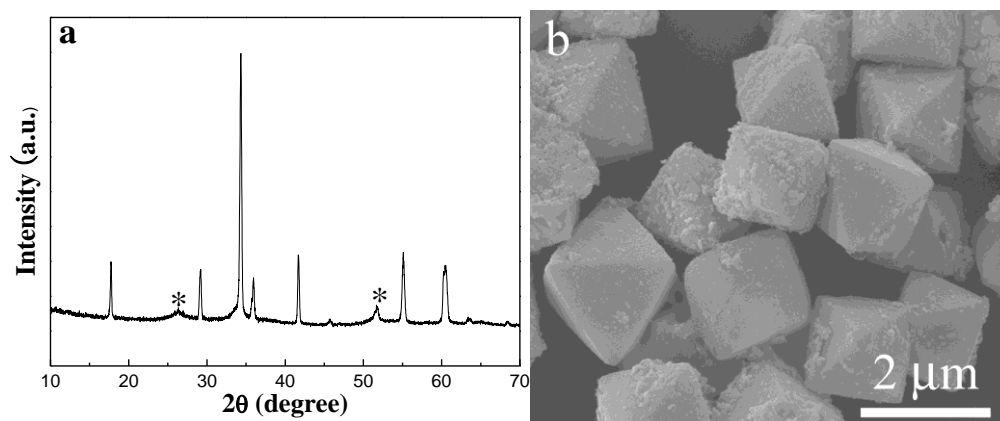


Figure S11. XRD pattern (a) and FE-SEM image (b) of Zn_2SnO_4 octahedrons hydrothermally treated in the presence of tartaric acid.

The XRD pattern of the resultant products can be indexed to main cubic-phase Zn_2SnO_4 (JCPDS no. 74-2184) and a small quantity of tetragonal-phase SnO_2 (denoted as *, JCPDS no. 88-0287). From EF-SEM image of the corresponding products, it can be seen that the products consist of octahedral microcrystals and a small quantity of nanoparticles.

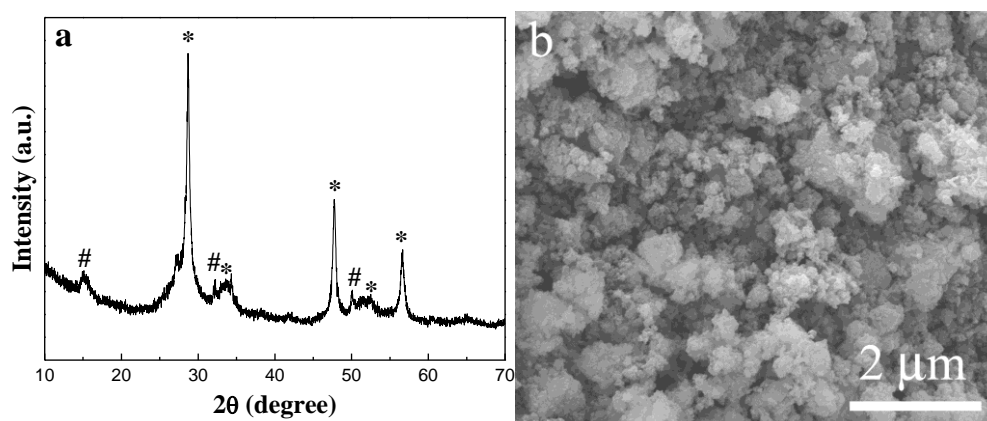


Figure S12. XRD pattern (a) and FE-SEM image (b) of the products synthesized with Zn_2SnO_4 octahedrons, TTA, and tartaric acid.

The XRD pattern of the resultant products can be indexed to main hexagonal-phase ZnS (denoted as *, JCPDS no. 89-2739) and a small quantity of hexagonal-phase SnS_2 (denoted as #, JCPDS no. 89-3198). From EF-SEM image of the corresponding products, it can be seen that the products consist of irregular particles.

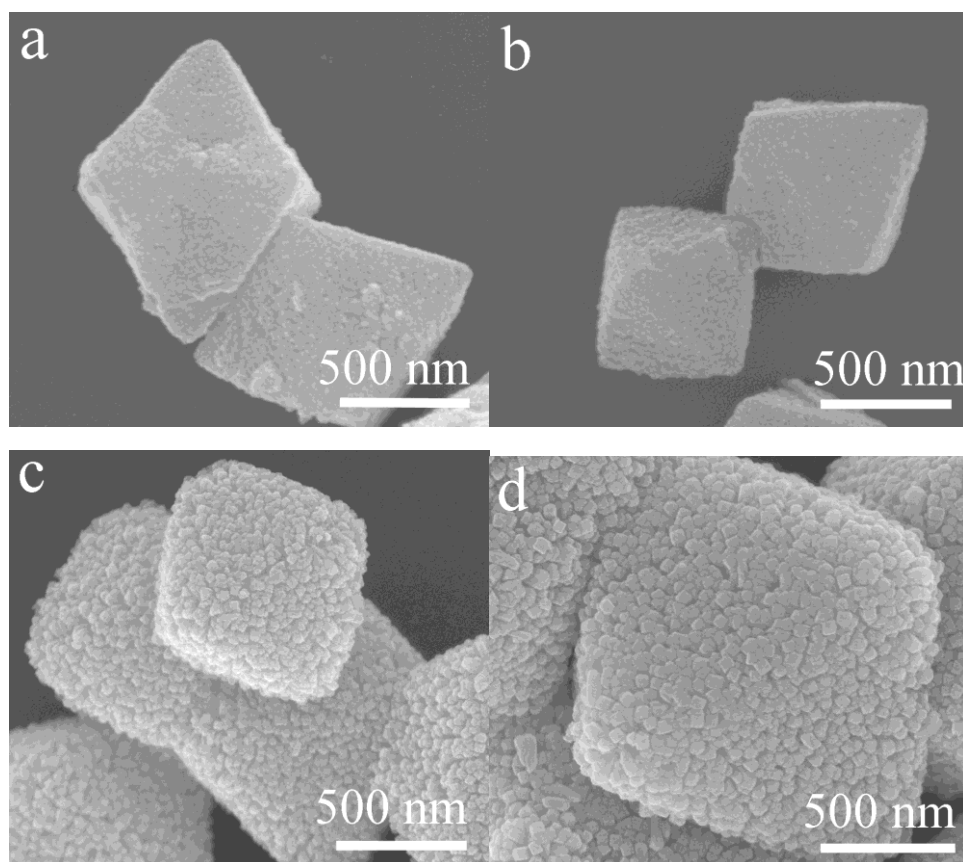


Figure S13. FE-SEM images of the intermediates at different reaction stages: (a) 0.5 h, (b) 1 h, (c) 4 h, and (d) 8 h.

As shown in Figure S13, the products still kept octahedral shape but with relatively rough surfaces after 0.5 h of hydrothermal reaction. Every octahedron consists of a lot of tiny nanoparticles. When reaction time was extended to 4 h, these nanoparticles obviously became bigger and were elongated at the same time. Up aging a longer period time up to 8 h, well-defined octahedrons assembled from nanorods were produced.

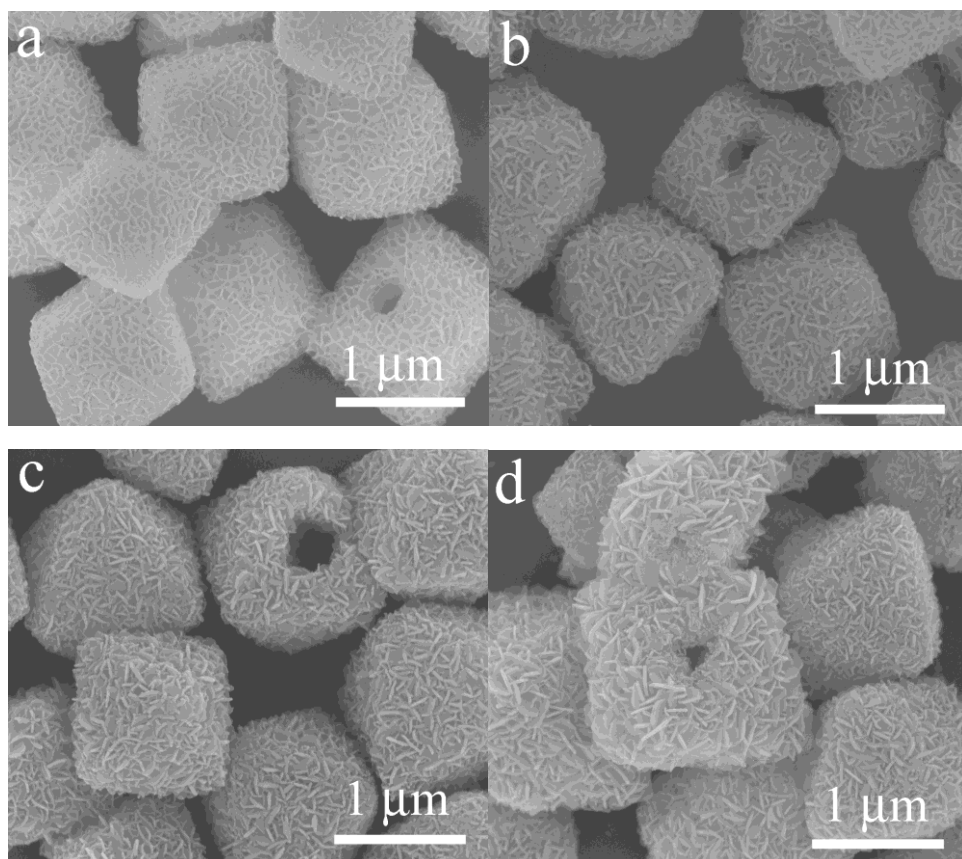


Figure S14. FE-SEM images of the intermediates at different reaction stages: (a) 0.5 h, (b) 1 h, (c) 2 h, and (d) 4 h.

As can be seen from Figure S14, the products have become hollow hierarchical octahedrons assembled from nanosheets after only 0.5 h of hydrothermal reaction. But, these nanosheets have not regular shapes at the moment. With increasing reaction time, these nanosheets would evolve into uniform ones with definite edges.

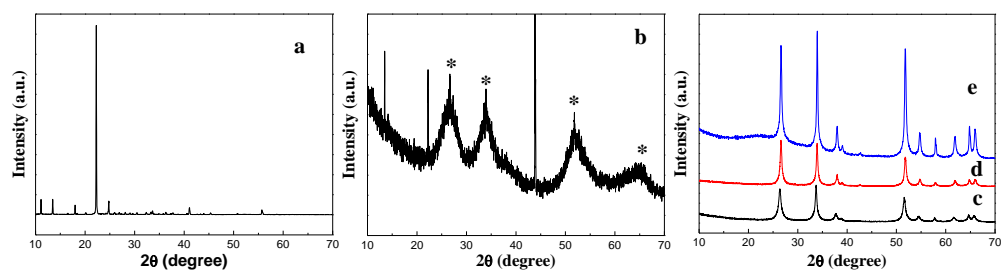
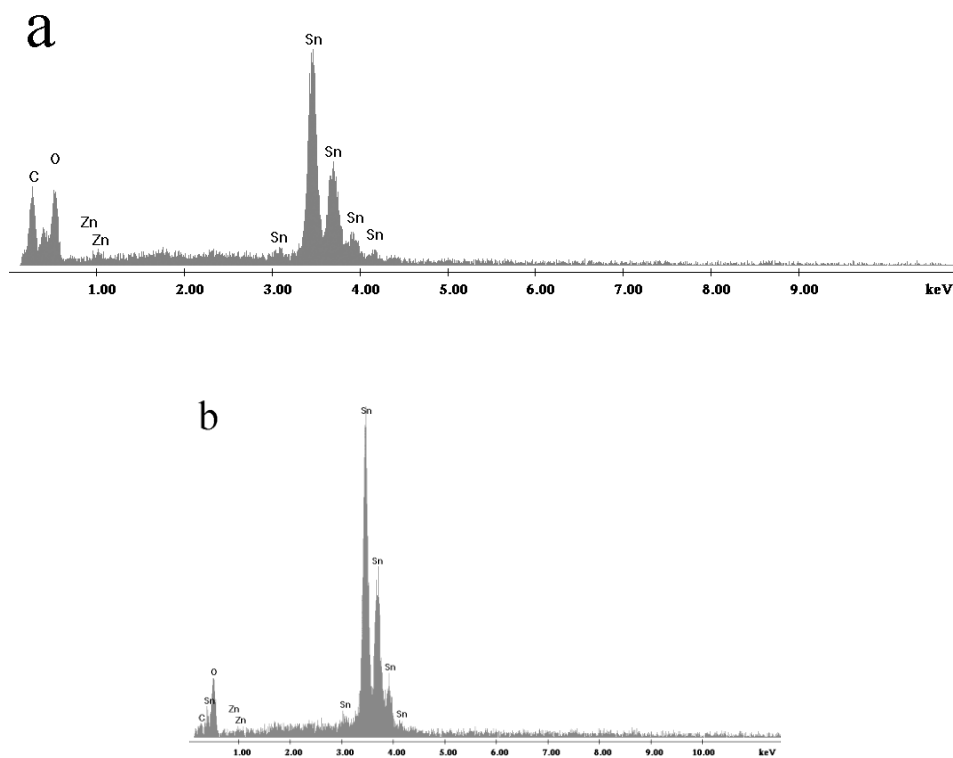


Figure S15. XRD patterns of the intermediates at different reaction stages: (a) 0.5 h, (b) 1 h, (c) 4 h, (d) 8 h, and (e) 12 h.

In Figure S15b, the diffraction peaks denoted as * can be indexed to tetragonal-phase SnO_2 (JCPDS no. 88-0287).



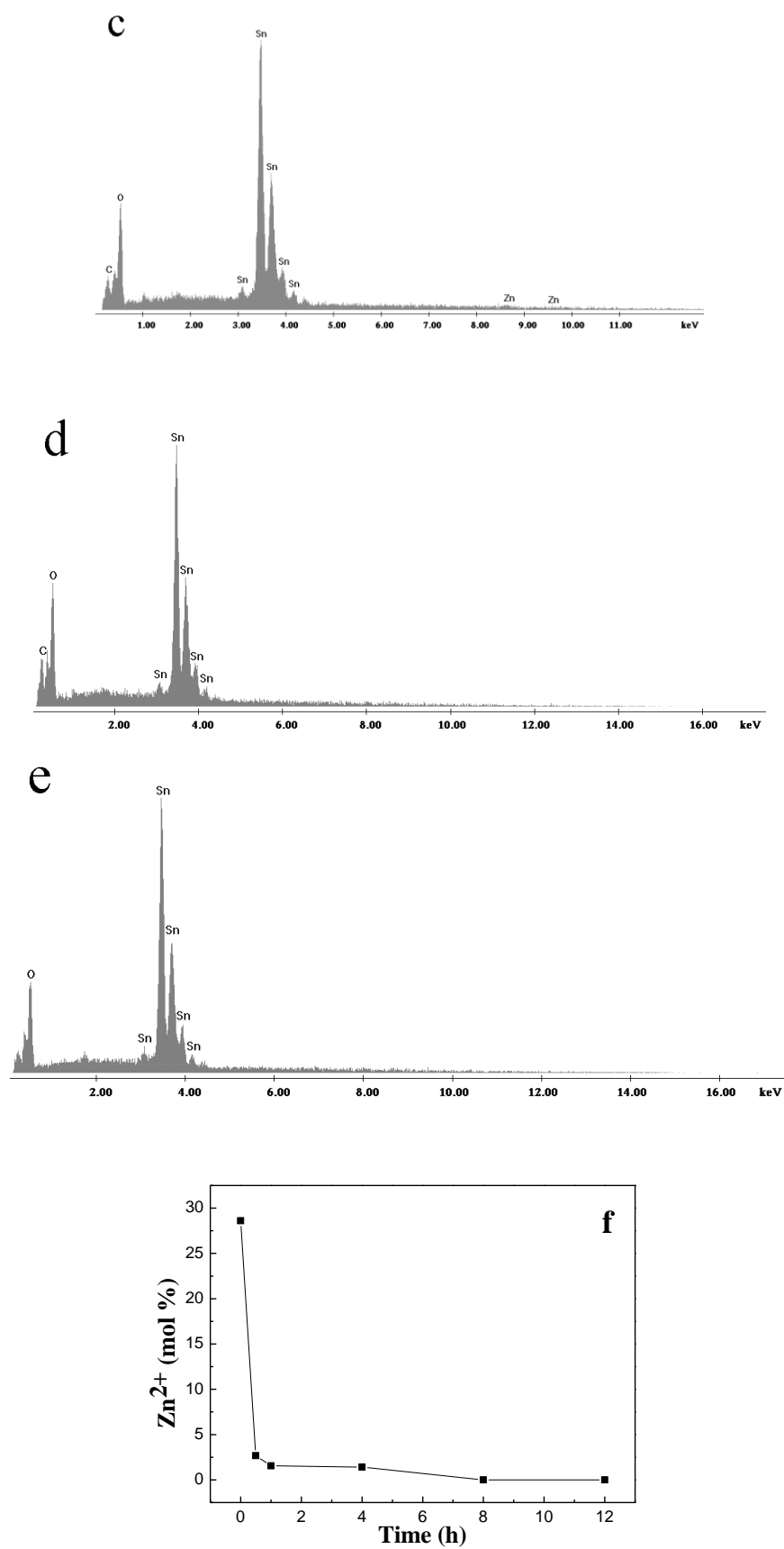


Figure S16. EDX spectra of the intermediates at different reaction stages: (a) 0.5 h, (b) 1 h, (c) 4 h, (d) 8 h, and (e) 12 h. Zn²⁺ ions content changes of the intermediate solid products as a function of reaction time (f).

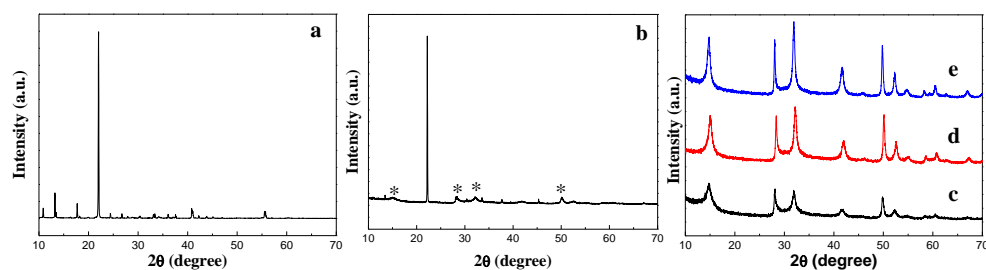
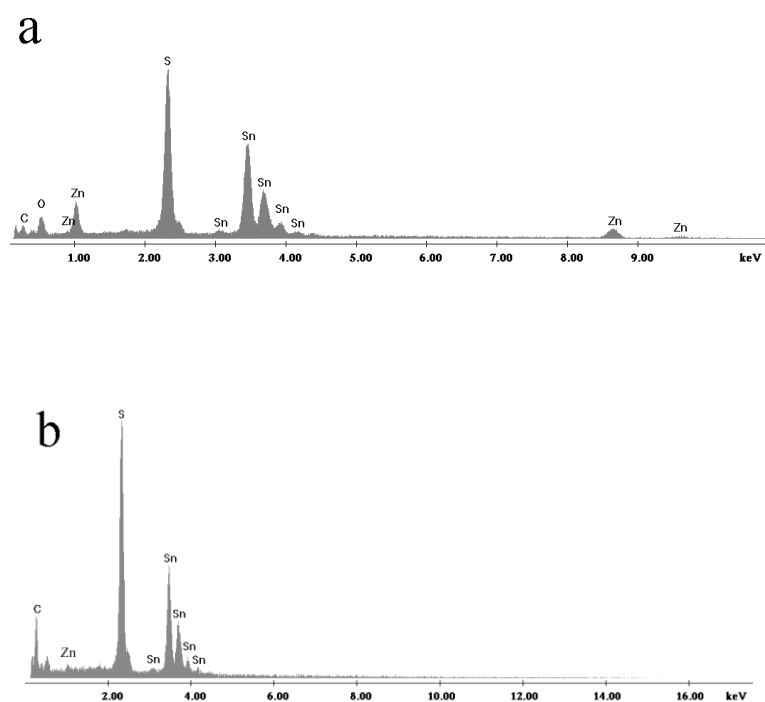


Figure S17. XRD patterns of the intermediates at different reaction stages: (a) 0.5 h, (b) 1 h, (c) 2 h, (d) 4 h, and (e) 8 h.

In Figure S17b, the diffraction peaks denoted as * can be indexed to hexagonal-phase SnS_2 (JCPDS no. 89-3198).



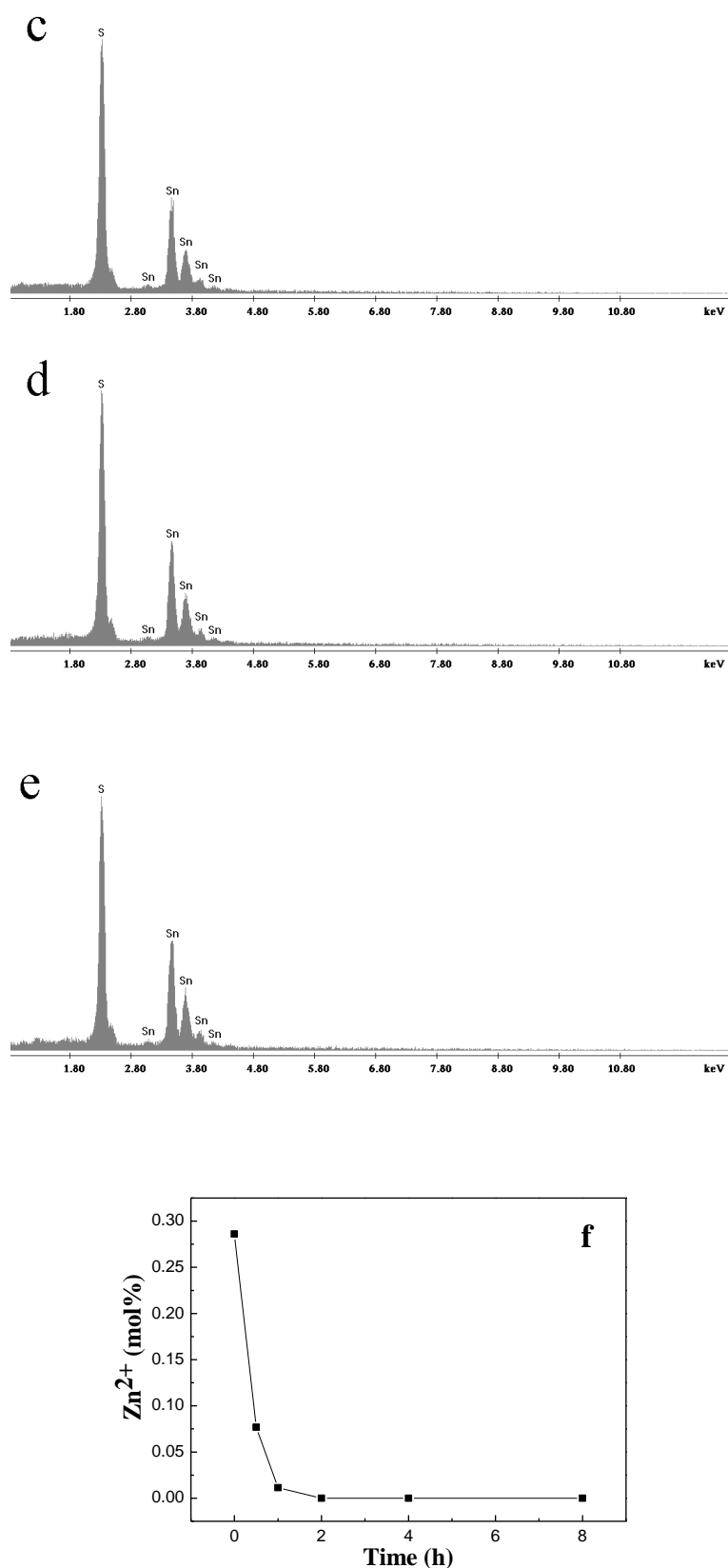


Figure S18. EDX spectra of the intermediates at different reaction stages: (a) 0.5 h, (b) 1 h, (c) 2 h, (d) 4 h, and (e) 8 h. Zn^{2+} ions content changes of the intermediate solid products as a function of reaction time (f).

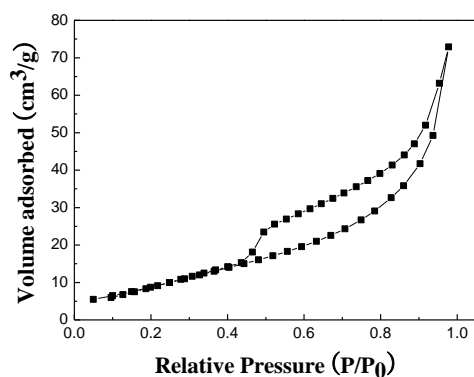


Figure S19. Nitrogen adsorption and desorption isotherms of hierarchical SnS₂ octahedrons (c).

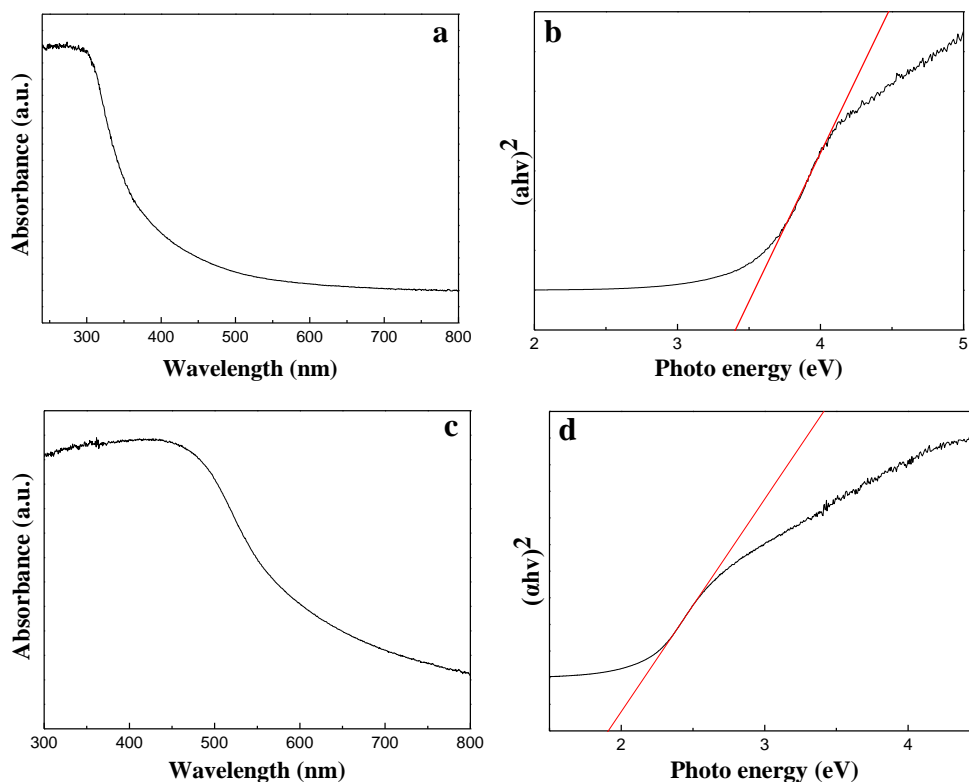


Figure S20. UV-visible DRS of (a) hierarchical SnO₂ octahedrons and (c) hierarchical SnS₂ octahedrons. Plots of $(\alpha h\nu)^2$ versus the photon energy ($h\nu$) of the-synthesized (b) hierarchical SnO₂ octahedrons and (d) hierarchical SnS₂ octahedrons.

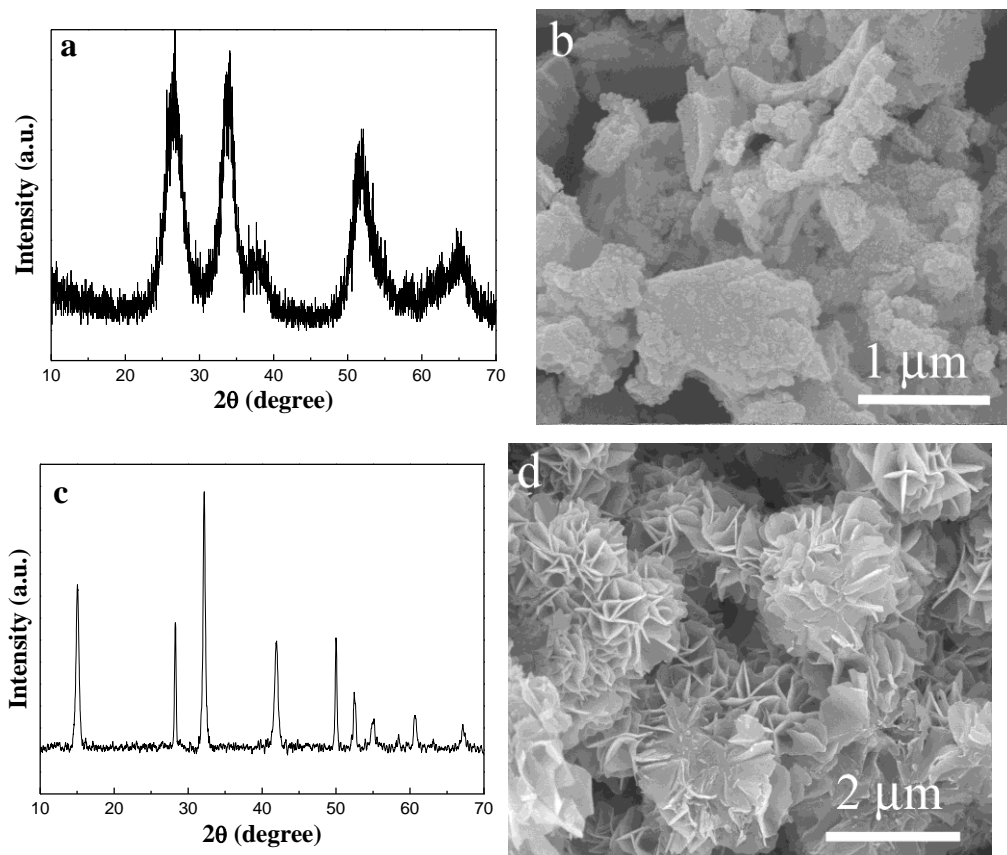


Figure S21. XRD pattern (a) and FE-SEM image (b) of SnO₂ synthesized by SSR method. XRD pattern (c) and FE-SEM image (d) of SnS₂ synthesized by SSR method.

The XRD pattern of the resultant products can be indexed to tetragonal-phase SnO₂ (Figure S21a, JCPDS no. 88-0287) and hexagonal-phase SnS₂ (Figure S21c, JCPDS no. 89-3198), respectively. From EF-SEM image of the corresponding products, it can be seen that SnO₂ products are conglomerations of tiny nanoparticles, which can be reflected by wide XRD diffraction peaks. SnS₂ shows hierarchical flower-like architectures assembled by nanosheets.

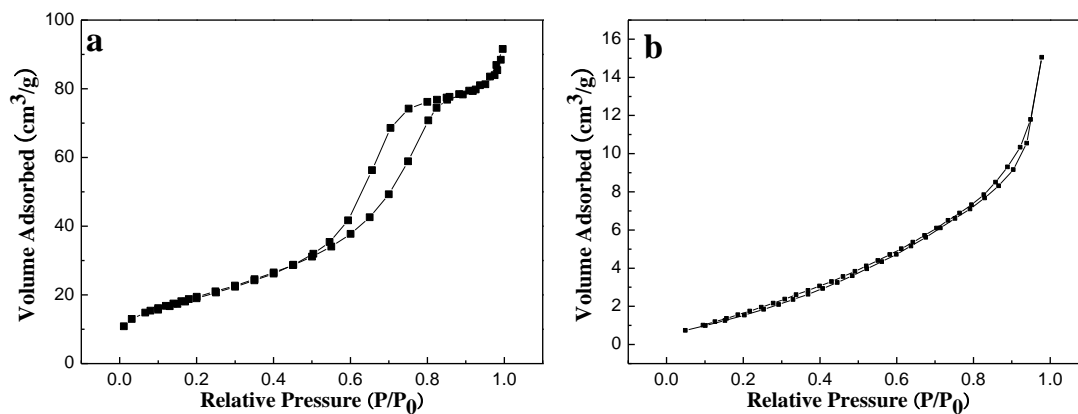


Figure S22. Nitrogen adsorption and desorption isotherms of (a) SnO₂ nanoparticles and (b) SnS₂ flowers obtained by SSR methods.

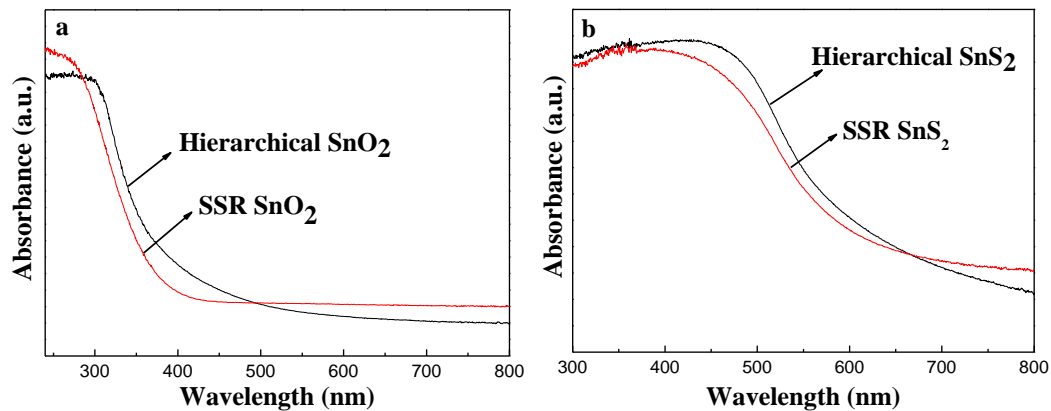


Figure S23. UV-visible absorption spectra of (a) hierarchical SnO₂ octahedrons and SnO₂ nanoparticles obtained through SSR method and (b) hierarchical SnS₂ octahedrons and SnS₂ flowers synthesized by SSR method.

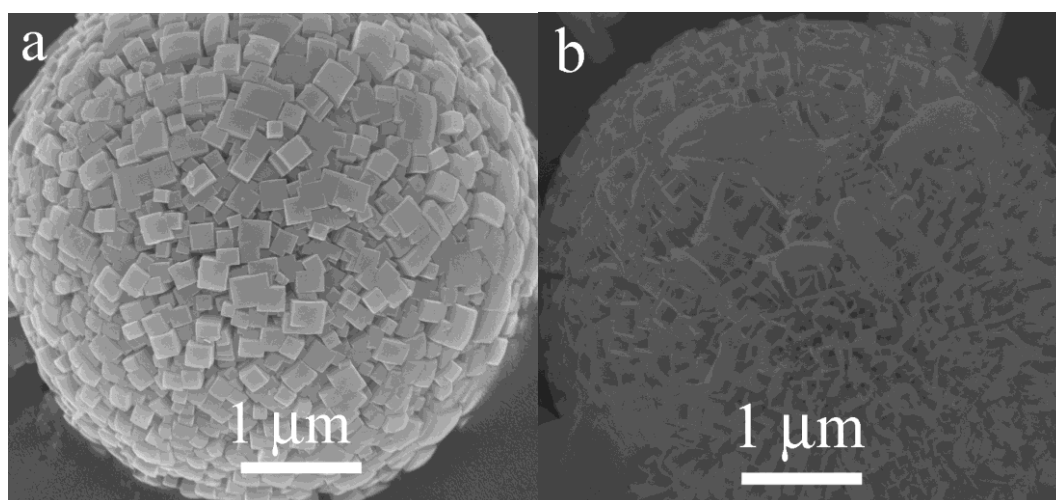


Figure S24. FE-SEM images of (a) the as-synthesized hierarchical Bi_2CuO_4 microspheres assembled by nanorods and (b) Bi_2O_3 nanotubes derived from selective extraction of Cu^{2+} ions in hierarchical Bi_2CuO_4 microspheres through complexing agent.